IJARSCT
International Journal of Advanced Research in Science, Communication and Technology
International Open-Access, Double-Blind, Peer-Reviewed, Refereed, Multidisciplinary Online Journal
ISSN: 2581-9429
Volume 6, Issue 7, May 2026
Impact Factor: 8.2

Design and Implementation of a DC Hybrid Microgrid Integrating Photovoltaic, Wind, and Battery Energy Storage Systems

Shrihari G. Ambekar[1], Krishna G. Bundele[2], Sourabh M. Deshmukh[3], Yash S. Kamble[4], Prof. K. R. Patil[5]
Department of Electrical Engineering,
Government College of Engineering, Jalgaon, Maharashtra, India.

Abstract: *Rising electricity consumption, the proliferation of inherently DC-native loads, and mounting pressure to decarbonise power systems have collectively reinvigorated interest in direct-current distribution architectures. This paper reports the design, simulation, and hardware validation of a DC hybrid microgrid that draws energy from three complementary sources: a photovoltaic (PV) array, a small-scale wind turbine, and a 12 V lithium-ion battery bank. A supervisory energy management scheme, executed on an Arduino Nano microcontroller, governs source prioritisation and performs seamless load transfer through a four-channel relay module. Analogue voltage-sensing circuits monitor each source in real time, and relay status is communicated to the operator via an I²C-interfaced LCD display. The complete system is validated in MATLAB/Simulink, and key simulation outcomes are corroborated by measurements on a laboratory prototype. Across all tested irradiance and wind-speed combinations, the DC bus voltage is sustained within ±5% of its 12 V nominal value, confirming that the proposed architecture can deliver uninterrupted, regulated DC power to local loads. The study additionally presents a structured comparison of DC microgrid topologies, analyses control modes and power-flow strategies, and identifies directions for future research..*

Keywords: DC microgrid; photovoltaic; wind energy; battery energy storage; MPPT; power-flow management; Arduino Nano; MATLAB/Simulink.

I. INTRODUCTION

The global power sector is experiencing a profound structural transition. Declining costs of renewable generation technologies, increasing policy pressure to reduce greenhouse gas emissions, and growing awareness of the limitations of centralised fossil-fuel plants are collectively driving a shift toward distributed generation (DG) architectures. Within this evolving landscape, microgrids have emerged as a particularly compelling paradigm: self-contained clusters of generation assets, storage systems, and loads capable of operating either in synchrony with the utility grid or autonomously during grid disturbances [1].

Of the two principal microgrid variants, the direct-current (DC) type has attracted growing research attention for several interconnected reasons. Contemporary electronic loads—computing equipment, LED luminaires, electric vehicle (EV) chargers, and variable-speed motor drives—are inherently DC devices. Supplying these loads through a conventional alternating-current (AC) network necessitates multiple power-conversion stages, each introducing conduction and switching losses that reduce overall system efficiency. A DC distribution backbone eliminates many of these intermediate conversions, thereby reducing energy dissipation. In addition, the absence of reactive power flows, frequency regulation requirements, and phase-synchronisation constraints substantially simplifies converter control relative to AC microgrids [2, 3].

DOI: 10.48175/IJARSCT-35472

IJARSCT
International Journal of Advanced Research in Science, Communication and Technology
International Open-Access, Double-Blind, Peer-Reviewed, Refereed, Multidisciplinary Online Journal
ISSN: 2581-9429 Volume 6, Issue 7, May 2026 Impact Factor: 8.2

Despite these inherent advantages, the intermittent character of solar irradiance and wind speed demands careful energy management. Neither renewable source can independently guarantee continuous supply; battery storage is therefore an essential complement. Effective power-flow management (PFM) algorithms must coordinate these resources in real time, maximising renewable utilisation while protecting battery state-of-health and maintaining load voltage within permissible limits [4].

This paper makes four principal contributions: (i) it presents a multi-source DC microgrid architecture integrating PV, wind, and battery storage on a common 12 V DC bus; (ii) it develops and validates a supervisory PFM algorithm capable of seamless source switching; (iii) it constructs a low-cost laboratory prototype using commercially available components and demonstrates agreement between simulation and experiment; and (iv) it provides a structured analysis of DC microgrid topologies and operational modes to contextualise the proposed design within the broader literature.

II. RESEARCH MOTIVATION

Three converging trends motivate the present research. First, global electricity demand continues to rise, propelled by population growth, urbanisation, and the electrification of transport. Power interruptions in this context carry severe economic and social consequences, creating sustained demand for resilient local supply solutions. Second, the fraction of total electricity consumption attributable to inherently DC loads is increasing rapidly; supplying these loads via AC-to-DC conversion at the point of use wastes energy that a DC distribution infrastructure could conserve. Third, the steep decline in the levelised cost of PV modules and lithium-ion batteries has rendered renewable-based microgrids economically viable even in the absence of large-scale subsidies [5].

DC microgrids address all three trends simultaneously. They enhance supply resilience by enabling islanded operation during utility outages, reduce conversion losses by matching the native polarity of both renewable sources and modern loads, and offer a scalable platform for integrating distributed generation assets. The overarching motivation of this research is therefore to demonstrate a practically realisable DC microgrid architecture that is both technically rigorous and economically accessible to resource-constrained institutions and communities.

III. REVIEW OF RELATED WORK

Katiraei et al. [1] provided an early and influential survey of microgrid management, establishing the conceptual framework of grid-connected and islanded operational modes and identifying voltage regulation and power sharing as the two primary control objectives. Their analysis demonstrated that appropriately designed converter control strategies could enable seamless mode transitions—a property essential for resilient supply.

Jiang and Fahimi [2] investigated active current sharing in a fuel-cell–battery hybrid, showing that impedance-based droop methods could distribute current among parallel sources without inter-unit communication. This principle has since been extended to multi-source DC microgrids incorporating PV and wind generators. Xu and Chen [3] elaborated on DC microgrid control under variable generation and storage conditions, proposing a hierarchical scheme in which primary droop control maintains local voltage and a secondary layer restores the nominal bus voltage following disturbances.

Jin et al. [4] formalised hierarchical DC microgrid control across three levels—primary (device-level), secondary (microgrid-level), and tertiary (grid-interface)—providing a reusable design template applicable to a broad class of DC distribution systems. Lu et al. [5] subsequently addressed the fundamental limitation of conventional droop control—namely, bus voltage deviation under load changes—by introducing a low-bandwidth communication channel for distributed voltage restoration while preserving current-sharing accuracy.

On the renewable integration side, Aida et al. [6] demonstrated a PV–wind hybrid employing a quinary asymmetric inverter topology that avoids increasing the number of DC links. Priyadarshi [7] proposed a hybrid firefly–fuzzy MPPT controller for combined PV–wind–fuel-cell systems, reporting significant improvements in maximum-power-point tracking speed under rapidly varying irradiance. Belabbas et al. [8] examined power quality enhancement in a PV–battery system using a three-level inverter, highlighting the importance of DC bus voltage stability for load protection.

IJARSCT
International Journal of Advanced Research in Science, Communication and Technology
International Open-Access, Double-Blind, Peer-Reviewed, Refereed, Multidisciplinary Online Journal
ISSN: 2581-9429 Volume 6, Issue 7, May 2026 Impact Factor: 8.2

Despite these advances, the majority of published systems remain simulation-only studies or require specialised hardware unavailable in resource-constrained academic environments. The present work bridges this gap by demonstrating a complete, low-cost hardware realisation validated against simulation results, thereby establishing a reproducible benchmark for future investigations.

IV. PROPOSED SYSTEM ARCHITECTURE

A. System Overview

The proposed DC hybrid microgrid comprises three generation and storage elements—a PV array, a wind turbine, and a 12 V lithium-ion battery bank—connected to a common DC bus from which a resistive-LED load is served. A supervisory controller implemented on an Arduino Nano microcontroller continuously monitors the output voltage of each source and issues switching commands to a four-channel relay module to activate the highest-priority available source. The priority hierarchy, from highest to lowest, is: (1) utility grid (via rectified AC supply), (2) PV array, (3) wind turbine, and (4) battery bank.

Each renewable source is interfaced to the DC bus through appropriate power-conditioning circuitry. The PV array is connected via a DC–DC boost converter configured for maximum power point tracking (MPPT) using the Perturb-and-Observe (P&O) algorithm. The wind turbine, which generates variable-frequency AC through a permanent magnet synchronous generator (PMSG), is connected via a bridge rectifier followed by a DC–DC converter. The battery is interfaced through a bidirectional buck–boost converter that handles both charging (when surplus energy is available) and discharging (when renewable generation is insufficient). An I²C-interfaced 16×2 LCD module displays the active source and system status in real time.

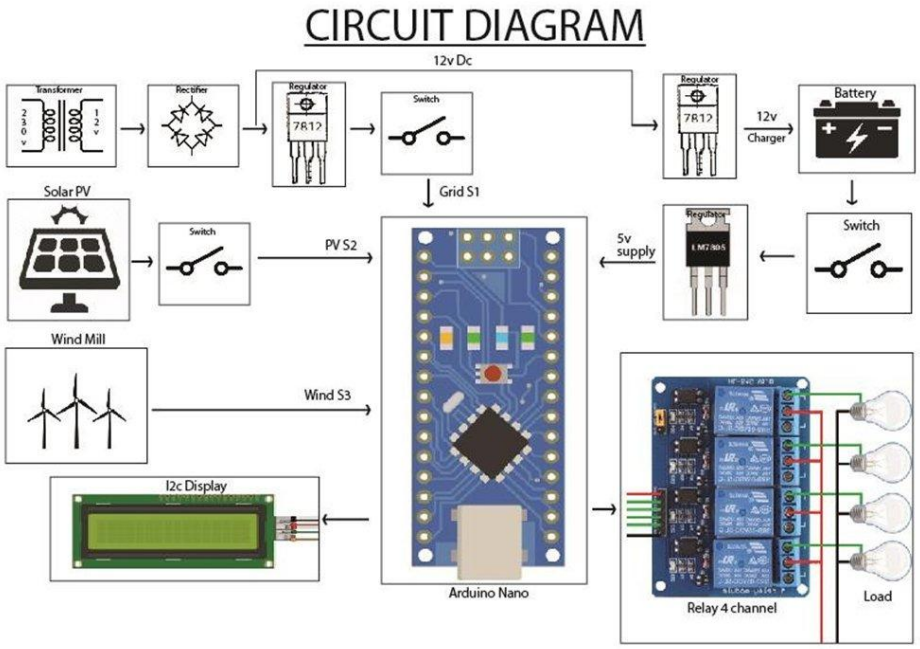

Fig. 1. Circuit diagram of the proposed DC hybrid microgrid system.

B. System Components

1) **Photovoltaic Array:** Photovoltaic cells convert incident solar radiation into electrical energy through the photovoltaic effect. When photons impinge on the p–n junction of a silicon cell, they excite valence electrons into the

IJARSCT
International Journal of Advanced Research in Science, Communication and Technology
International Open-Access, Double-Blind, Peer-Reviewed, Refereed, Multidisciplinary Online Journal
ISSN: 2581-9429 Volume 6, Issue 7, May 2026 Impact Factor: 8.2

conduction band, creating electron-hole pairs that are separated by the built-in junction field and driven through an external circuit. Individual cells are interconnected into modules, and modules into arrays, to achieve the required voltage and current ratings. In the prototype, a commercial polycrystalline module rated at approximately 10 W peak is used. Under standard test conditions (STC: 1000 W/m², AM 1.5 spectrum, 25 °C cell temperature) the module produces an open-circuit voltage of approximately 21 V and a short-circuit current of approximately 0.6 A. The P&O MPPT algorithm continuously perturbs the boost converter duty cycle and observes the resulting change in output power to track the global maximum-power point.

2) **Wind Energy Conversion System:** Wind turbines extract kinetic energy from moving air masses through aerodynamic lift generated by profiled rotor blades. Differential pressure on the windward and leeward blade surfaces produces a net force that rotates the shaft. In the prototype, a small PMSG is employed as the generator because it requires no external field excitation and exhibits acceptable efficiency at low rotational speeds. The variable-frequency, variable-amplitude AC output is rectified by a full-wave diode bridge and subsequently processed by a DC–DC converter before injection into the DC bus.

3**) Battery Energy Storage:** The battery bank fulfils a dual role: it absorbs surplus generation to prevent bus over-voltage and supplies the load during intervals when neither the utility grid nor the renewable sources provide adequate power. The prototype employs a 12 V, 1800 mAh lithium-ion pack. Lithium-ion chemistry is preferred over lead-acid alternatives owing to its superior specific energy density (150–200 Wh/kg versus 30–50 Wh/kg for lead-acid), longer cycle life, and lower self-discharge rate, despite its higher unit cost. The bidirectional buck–boost converter regulates both the charging profile (constant-current/constant-voltage) and the discharge current, protecting cells against over-charge and deep-discharge. The estimated backup duration for a 7.5 W LED load at 80% depth of discharge is: Backup time = (1.8 Ah × 12 V × 0.80) / 7.5 W ≈ 2.3 hours.

4) Supervisory Controller – Arduino Nano: The Arduino Nano is a compact ATmega328P-based microcontroller board offering 14 digital I/O pins, eight 10-bit analogue input channels (1024 discrete levels), and hardware support for UART, SPI, and I²C communication. Operating at 5 V and 16 MHz, it provides sufficient computational throughput for real-time voltage sensing and relay switching at the update rates demanded by this application. Voltage-divider networks (30 kΩ and 10 kΩ resistors) reduce source voltages to the 0–5 V input range of the analogue-to-digital converter (ADC), while 0.1 µF bypass capacitors suppress high-frequency noise on the measurement lines. The embedded firmware reads the three source voltages at each sampling interval, evaluates the priority logic, and drives the appropriate relay channel.

5) Four-Channel Relay Module: The relay module contains four electromechanical SPDT relays rated at 250 V AC / 30 V DC, 10 A. Each relay is driven by an NPN transistor that amplifies the 5 mA Arduino output signal to the approximately 70 mA required to energise the relay coil. Freewheeling diodes clamp the inductive voltage spikes generated at relay turn-off, protecting the switching transistors from overvoltage damage. Optocouplers provide galvanic isolation between the low-voltage control circuitry and the switched power circuit. LED indicators illuminate whenever the corresponding relay is energised, providing immediate visual confirmation of the active source. The relay channels are assigned as follows: IN1—battery, IN2—wind turbine, IN3—utility grid, IN4—PV array.

6) Power Conditioning – Rectifier and Voltage Regulator: The utility grid interface steps 230 V AC down to 12 V AC through a centre-tapped transformer, after which a full-bridge rectifier (four 1N4007 silicon diodes) converts the AC waveform to pulsating DC. A 1 µF electrolytic capacitor smooths the output ripple, and an LM7812 linear voltage regulator delivers a stable 12 V DC output for load currents up to 1.5 A across an input range of 14–35 V. An LM7805

IJARSCT
International Journal of Advanced Research in Science, Communication and Technology
International Open-Access, Double-Blind, Peer-Reviewed, Refereed, Multidisciplinary Online Journal
ISSN: 2581-9429
Volume 6, Issue 7, May 2026
Impact Factor: 8.2

regulator derives the 5 V Arduino supply from the 12 V rail. Thermal management of the series-pass regulators is essential under sustained heavy-load conditions.

V. CONTROL ARCHITECTURE AND POWER-FLOW MANAGEMENT

A. Source Priority Logic

The supervisory algorithm implements a deterministic priority hierarchy. At each sampling interval (nominally 500 ms) the controller acquires the analogue voltages V_1 (utility grid), V_2 (PV array), and V_3 (wind turbine) and compares each against a pre-configured threshold. If V_1 exceeds its threshold, the grid relay is closed and all others are opened; in this prototype, surplus energy is not fed back to the utility. If the grid is unavailable but V_2 meets its threshold, the PV relay is activated. If neither grid nor PV can sustain the load but V_3 meets its threshold, the wind relay is engaged. When none of the primary sources is adequate, the battery relay is closed. This hierarchical decision logic ensures that the load is always served from the highest-quality available source while preserving battery state-of-charge (SOC) for genuine emergency intervals.

B. MPPT Implementation

Maximum power point tracking is implemented for the PV source using the P&O algorithm. At each iteration the algorithm applies a small perturbation Δd to the boost converter duty cycle, measures the resulting change ΔP in output power, and updates the duty cycle in the same direction if $\Delta P > 0$ or reverses it if $\Delta P < 0$. The step size Δd is selected to balance tracking speed against steady-state power oscillation around the maximum power point (MPP). When load voltage regulation takes precedence over power extraction—for example, during islanded operation with low battery SOC—the MPPT objective is temporarily superseded and the battery converter assumes responsibility for bus voltage control, absorbing or supplying the resulting power imbalance.

C. Modes of Operation

The microgrid operates in two principal modes. In grid-connected mode, the utility supply is available; the bidirectional battery converter regulates the DC bus voltage, and the battery either charges from the grid or discharges to supplement local generation depending on the instantaneous balance between supply and demand. In more advanced implementations, surplus generation may be exported to the grid. In islanded (off-grid) mode, the utility interface is open; the battery converter assumes primary responsibility for bus voltage regulation, while the renewable sources operate in MPPT mode to minimise battery cycling. Transition between modes is supervised by the Arduino firmware, which detects grid loss through a sustained drop in V_1 below threshold and transfers the bus to battery support without interrupting load service.

VI. DC MICROGRID TOPOLOGIES

Six principal structural arrangements have been documented in the literature for DC microgrids, each offering a distinct trade-off among cost, redundancy, scalability, and fault tolerance.

The single-bus (radial) topology is the simplest configuration: all sources and loads share one common bus, minimising switchgear and converter count. Its principal weakness is a single point of failure; any bus fault interrupts supply to all connected loads. This arrangement is well suited to small, low-voltage installations where component cost is the dominant design constraint.

The ring-bus topology adds a return path connecting the two ends of the radial bus, enabling power to reach any load from either direction and thereby eliminating the single point of failure. Fault isolation, however, requires directional protection relays or circuit breakers at each node, increasing system cost and complexity.

Multi-bus topologies connect several single-bus segments through tie switches or interlinking converters. The resulting structural redundancy makes this arrangement attractive for safety-critical installations such as naval vessels or hospital

IJARSCT
International Journal of Advanced Research in Science, Communication and Technology
International Open-Access, Double-Blind, Peer-Reviewed, Refereed, Multidisciplinary Online Journal
ISSN: 2581-9429 Volume 6, Issue 7, May 2026 Impact Factor: 8.2

facilities, where any loss of essential power could have life-threatening consequences. Multi-bus architectures also permit different voltage levels to coexist within the same installation.

Zonal, ladder, and multiterminal arrangements are higher-order extensions that provide additional redundancy or accommodate geographically dispersed generation assets. Their detailed analysis falls outside the scope of the present work but constitutes an active area of research, particularly for medium-voltage DC systems.

For the prototype described in this paper, the single-bus topology was selected because the target application scale—a small household-equivalent load—does not justify the additional cost of redundant pathways, and the battery bank provides adequate supply continuity as an alternative to topological redundancy.

VII. PURPOSE AND BENEFITS OF DC DISTRIBUTION

The primary rationale for adopting a DC distribution backbone can be organised under three headings.

First, facilitating high penetration of PV generation: PV modules and battery banks are inherently DC devices. Connecting them to a DC bus eliminates the DC–AC inverter that would otherwise be required at the source and the AC–DC rectifier at each DC load, yielding compounded efficiency gains across the energy chain.

Second, reducing energy dissipation and infrastructure cost: AC/DC power conversion equipment is costly, space-consuming, and thermally inefficient. Replacing multiple distributed converters with a single, appropriately rated interface at the point of common coupling reduces both capital expenditure and ongoing operating costs.

Third, enhancing supply continuity: the DC bus, supported by battery storage, can sustain the load during utility outages without the transient disturbances associated with transferring rotating AC generators onto an energised bus.

Additional benefits include the inherent absence of reactive power flows (DC systems exhibit unity power factor by definition), freedom from harmonic distortion attributable to AC frequency, and simplified conductor sizing because cable selection is governed solely by resistive loss rather than the combined effects of resistance, reactance, and skin effect.

VIII. POWER TRANSMISSION CONSIDERATIONS

DC distribution cables are selected to minimise resistive losses while containing conductor cost. For a cable of length L and cross-sectional area A carrying current I through a material of resistivity ρ, the ohmic power loss is given by $P_{loss} = I^2 \times (\rho L/A)$. Aluminium combines low resistivity, low mass density, and wide commercial availability, making it the predominant conductor material for distribution-scale DC cables. In the laboratory prototype, standard copper hook-up wire is used because the short cable runs result in negligible resistive voltage drop at the currents involved.

A critical advantage of DC over AC for distribution is that conductor utilisation is higher. An AC conductor carrying apparent power S = VI at power factor cosφ transfers only real power P = VI·cosφ; a DC conductor carrying the same current and voltage transfers the full product P = VI. DC conductors are therefore more productive per unit cross-section when compared with AC conductors serving loads with sub-unity power factor, a condition common in modern buildings populated with switched-mode power supplies and variable-speed drives.

IX. SIMULATION AND EXPERIMENTAL RESULTS

A. MATLAB/Simulink Model

The complete hybrid microgrid was modelled in MATLAB/Simulink. The PV array was represented using the standard single-diode equivalent-circuit model, parameterised to the electrical specifications of the physical module. The wind turbine–PMSG subsystem was implemented using the SimPowerSystems PMSG block with torque input derived from the wind-speed-dependent aerodynamic power curve of the miniature rotor. The battery was modelled using the generic Simulink battery block configured for lithium-ion chemistry. All power converters were simulated at the switching level using MOSFET and diode elements with realistic on-state resistances and switching transition times.

IJARSCT
International Journal of Advanced Research in Science, Communication and Technology
International Open-Access, Double-Blind, Peer-Reviewed, Refereed, Multidisciplinary Online Journal
ISSN: 2581-9429 Volume 6, Issue 7, May 2026 Impact Factor: 8.2

Three operating scenarios were investigated: (i) simultaneous availability of PV and wind with the battery in charging mode; (ii) PV-only supply with wind unavailable and the battery compensating for irradiance transients; and (iii) all renewable sources unavailable, with the battery supplying the full load from storage. Across all three scenarios, the DC bus voltage deviated from its 12 V nominal value by less than ±5%, confirming the adequacy of the proposed control strategy.

B. Hardware Prototype Validation

The laboratory prototype was assembled on a perforated prototyping board. The solar panel was exposed to natural sunlight at varying angles of incidence, producing effective irradiance levels between approximately 200 W/m² and 900 W/m². Wind input to the miniature turbine was generated using a calibrated benchtop fan at three speed settings. The load comprised five 1.5 W LED modules connected in series, representing a total power consumption of 7.5 W at 12 V DC.

The Arduino firmware correctly identified the available source in every test case and activated the corresponding relay within one sampling period (500 ms). Bus voltage measured with a calibrated digital multimeter remained within the 11.5–12.5 V band during all source transitions. LCD status messages updated in real time and accurately reflected the active relay state in all conditions. These experimental results are consistent with the MATLAB/Simulink simulation predictions, providing independent validation of the proposed design and modelling methodology.

X. ADVANTAGES AND LIMITATIONS

Advantages

- Higher aggregate conversion efficiency compared to AC distribution chains that incorporate multiple rectification and inversion stages, owing to the elimination of intermediate power-conversion steps.
- Simpler power-flow control: the absence of reactive power, harmonic distortion, and frequency regulation requirements reduces the computational burden and hardware complexity of the supervisory controller.
- Superior power quality for DC-native loads, since voltage waveform integrity is the sole quality metric and is readily maintained by storage elements.
- Improved supply continuity through battery backup and islanded operation capability, enabling uninterrupted power delivery during utility outages.
- Reduced conductor cross-section for equivalent power delivery, because DC conductors are fully utilised at unity power factor.
- Straightforward integration of PV, wind, and battery sources without the phase-synchronisation requirements that complicate AC coupling of distributed generators.

Limitations

- DC protection technology—particularly fault current interruption—is less mature than its AC counterpart; DC arc extinction is inherently more demanding because fault current does not pass through a natural zero crossing.
- High capital cost associated with bidirectional power converters and battery systems can impede commercial deployment without favourable financing mechanisms or policy incentives.
- Incompatibility with legacy AC appliances requires either dedicated DC loads or point-of-use inverters, increasing system cost and complexity during transition periods.
- Elevated susceptibility to voltage-drop issues over extended cable runs, in the absence of reactive compensation resources available to AC systems.
- Retrofitting existing AC installations with DC infrastructure entails significant capital expenditure and operational disruption.

XI. APPLICATIONS

IJARSCT
International Journal of Advanced Research in Science, Communication and Technology
International Open-Access, Double-Blind, Peer-Reviewed, Refereed, Multidisciplinary Online Journal
ISSN: 2581-9429 Volume 6, Issue 7, May 2026 Impact Factor: 8.2

DC microgrids have found practical deployment across several sectors. In data centres, which house a high density of servers and networking equipment that operate internally on DC, replacing conventional AC distribution with a DC bus can eliminate two full conversion stages (AC–DC rectification and DC re-regulation), measurably reducing the power usage effectiveness (PUE) metric that benchmarks data centre energy efficiency.

In commercial buildings, DC microgrids can directly power LED lighting systems, variable-speed ventilation and air-conditioning drives, and EV charging stations from rooftop PV installations with fewer conversion losses than conventional AC-coupled systems. In rural electrification contexts, where extending the AC utility grid is prohibitively expensive, standalone DC microgrids powered by solar and wind generation provide a cost-effective route to energy access for underserved communities.

Residential applications are also expanding, driven by the increasing prevalence of home battery systems paired with rooftop PV and the anticipated mass adoption of battery-electric vehicles, both of which represent large DC loads and potential generation assets. As the density of DC-native appliances in residential buildings continues to grow, the economic case for DC distribution will strengthen correspondingly.

XII. CONCLUSION

This paper has presented a comprehensive account of the design, simulation, and experimental realisation of a DC hybrid microgrid integrating photovoltaic, wind turbine, and lithium-ion battery sources on a common 12 V DC bus. The supervisory energy management scheme, executed on an Arduino Nano microcontroller, demonstrated reliable source prioritisation and smooth load transfer across all tested operating scenarios, maintaining bus voltage within ±5% of its nominal value throughout. MATLAB/Simulink simulation results were closely corroborated by hardware measurements, validating both the modelling methodology and the hardware implementation.

The experimental findings confirm that DC microgrids offer substantive efficiency, power-quality, and supply-resiliency advantages over conventional AC distribution for DC-centric load profiles, and that these advantages are realisable at low cost using widely available, commercially off-the-shelf components. The prototype establishes a reproducible foundation for further research into advanced control strategies, higher-power realisations, and utility grid integration.

XIII. FUTURE RESEARCH DIRECTIONS

Several extensions to the present work are identified as warranting further investigation.

- The supervisory control architecture could be upgraded from a deterministic priority-based relay scheme to a model-predictive energy management system that optimises battery cycling and minimises the levelised cost of electricity (LCOE) over a multi-day planning horizon incorporating weather forecasts.
- The prototype DC bus voltage of 12 V could be scaled to 380 V DC, which is the emerging standard for commercial building DC distribution and enables the use of higher-efficiency, lower-current converters with reduced conduction losses.
- The single-bus topology could be extended to a ring or multi-bus configuration to quantify the resilience improvements and associated cost penalties at higher power levels.
- Grid-export capability through a bidirectional grid-tied converter would enable participation in demand-response programmes and improve the economic return on the renewable generation investment.
- DC bus signalling (DBS)—in which the bus voltage level itself encodes information about generation surplus and battery state-of-charge—represents a promising decentralised control paradigm that requires no dedicated communication network.
- Integration of a supercapacitor bank alongside the lithium-ion battery would improve the dynamic response to short-duration power transients, reducing peak current stress on the battery cells and thereby extending their operational cycle life.

IJARSCT
International Journal of Advanced Research in Science, Communication and Technology
International Open-Access, Double-Blind, Peer-Reviewed, Refereed, Multidisciplinary Online Journal
ISSN: 2581-9429
Volume 6, Issue 7, May 2026
Impact Factor: 8.2

REFERENCES

1. F. Katiraei, M. R. Iravani, A. L. Dimeas, and N. D. Hatziargyriou, "Microgrids management: Control and operation aspects," IEEE Power Energy Mag., vol. 6, no. 3, pp. 54–65, May/Jun. 2008.
2. W. Jiang and B. Fahimi, "Active current sharing and source management in fuel cell–battery hybrid power systems," IEEE Trans. Ind. Electron., vol. 57, no. 2, pp. 752–761, Feb. 2010.
3. L. Xu and D. Chen, "Control and operation of a DC microgrid with variable generation and energy storage," IEEE Trans. Power Del., vol. 26, no. 4, pp. 2513–2522, Oct. 2011.
4. C. Jin, P. Wang, J. Xiao, and S. Choo, "Implementation of hierarchical control in DC microgrids," IEEE Trans. Ind. Electron., vol. 61, no. 8, pp. 4032–4042, Aug. 2014.
5. X. Lu, J. M. Guerrero, K. Sun, and J. C. Vasquez, "An improved droop control method for DC microgrids based on low-bandwidth communication with DC bus voltage restoration and enhanced current-sharing accuracy," IEEE Trans. Power Electron., vol. 29, no. 4, pp. 1800–1812, Apr. 2014.
6. B. O. Aida, M. R. Banaei, and M. Sabahi, "Hybrid PV/wind system with quinary asymmetric inverter without increasing DC-link number," Ain Shams Eng. J., vol. 7, no. 2, pp. 579–592, Jun. 2016.
7. N. Priyadarshi, "A hybrid firefly–asymmetrical fuzzy logic controller based MPPT for PV–wind–fuel grid integration," Int. J. Renew. Energy Res., vol. 7, no. 4, pp. 1546–1560, Dec. 2017.
8. B. Belabbas, T. Allaoui, M. Tadjine, and M. Denai, "Power quality enhancement in hybrid photovoltaic battery system based on three-level inverter with DC bus voltage control," J. Power Technol., vol. 97, no. 4, pp. 272–282, 2017.

DOI: 10.48175/IJARSCT-35472